Avicenna J Environ Health Eng. 2017 June; 4(1):e61902. doi: 10.5812/ajehe.61902.

Published online 2017 June 30. **Research Article**

Preparation of Magnetic Multi-Walled Carbon Nanotubes to Adsorb Sodium Dodecyl Sulfate (SDS)

Zahra Rahmani,[1] and Mohammad Taghi Samadi[1,*]

[1]Department of Environmental Health Engineering, Faculty of Health, Hamedan university of Medical Sciences, Hamedan, IR Iran

[*]*Corresponding author*: Mohammad Taghi Samadi, Department of Environmental Health Engineering, Faculty of Health, Hamedan University of Medical Sciences, Hamedan, IR Iran. Tel: +98-9188129968, Fax: +98-08138380025, E-mail: samadi@umsha.ac.ir

Received 2017 April 17; **Accepted** 2017 May 22.

Abstract

Surfactants are one of the main groups of pollutants released into aqueous solutions due to human activities and their harmful effects have been proven on human. In this study, first, magnetic multi-walled carbon nanotubes (MMWCNTs) were synthesized and then, the effects of operating parameters such as surfactant concentration, adsorbent dosage, and pH values were analyzed on the adsorption process. MMWCNTs were characterized by means of X-ray diffraction (XRD) analysis and fourier transform infrared spectroscopy (FTIR). The optimal adsorption conditions were achieved at initial pH = 4.6, adsorbent concentration = 0.5 g/L, and initial SDS concentration = 15 mg/L. In addition, the equilibrium of sorption reached after 120 min and the maximum capacity of SDS for monolayer coverage was found to be 61 mg/g at 25°C. Kinetic studies were performed under optimal conditions and the sorption kinetics was described using the pseudo-second-order kinetic model. The experimental data were studied using Freundlich, Langmuir, and Sips models. Finally, the experimental data were fitted reasonably by Langmuir isotherm. The results demonstrated that MMWCNTs with respect to their high adsorption capacity, relatively low equilibrium time, and capability to be separated from aqueous solutions (after adsorption) could be applied to wastewater treatment.

Keywords: Sodium Dodecyl Sulfate (SDS), Magnetic Multi-Walled Carbon Nanotubes (MMWCNTs), Adsorption, Kinetics and Isotherms

1. Introduction

Development of industries and consequently industrial wastewater discharge into the environment has caused a large number of concerns due to surface and groundwater pollution and environmental destruction (1, 2). Surfactants are one of the main groups of pollutants released to aqueous solutions by humankind. In other words, surfactants are known to implicate in the increment of hazardous contaminants. Due to the extensive use of surfactants in today's world, they can be found in a wide range of daily products such as soaps, detergents, pharmaceutical products, personal care products, as well as in industries including high-technology equipment, painting, and leather products. Hence, the release of these kinds of contaminants to aqueous solutions is inevitable (3, 4). According to the ionic characteristics, surfactants are divided into several types including: anionic, cationic, amphoteric, and nonionic. SDS is one of the typical anionic surfactants that may accumulate in the human body (5-7).

Employing approaches such as ozonation in order to remove surfactants in large scales is completely difficult and costly. Additionally, due to strong germicidal effects of surfactants, application of biological methods to get rid of these contaminants in high concentrations is almost impossible (8). Therefore, it seems that adsorption is one of the best methods, which can easily remove pollutants; moreover, it is more practical than other old techniques are. Currently, the consumption of nanoparticles to adsorb pollutants has drawn scientists' attention. Certainly, if carbon nanotubes (CNTs) are made up of single-walled (SWCNTs) or multi-walled (MWCNTs) carbon nanotubes, they will really be applicable adsorbents. CNTs as novel adsorbents have increasingly attracted attention of numerous researchers because of their small size, high surface area, crystalline form, unique organized lattice, and acceptable reactivity (9). It can be used to treat wastewater and transform pollutants to less harmful substances (10, 11). Indeed, CNTs have gotten the world's attention because of their ability to separate contaminants like heavy metals (12-14), radio nucleotides, hazardous organics, and inorganic compounds (15, 16).

Gao et al. successfully obtained magnetic polymer multi-walled carbon nanotube nanocomposite, which could adsorb anionic azo dyes. The results demonstrated that the efficiency of dye adsorption was 90% at acidic pH. The results also showed that adsorption of the mentioned contaminant followed Langmuir isotherm and reaction kinetic followed the pseudo-second order model

(17). Tang et al. could separate atrazine and copper ions from aqueous solutions using MMWCNTs with efficiency of 90%. The results revealed that adsorption efficiency decreased at acidic pH and reaction kinetics pursued the pseudo-second order equation. Recovery of MMWCNTs adsorbent was possible within a multi-cycle process. The adsorbents could easily be separated from the aqueous solution using a magnetic field (18). Konicki et al. investigated the performance of MMWCNTs for separation of anionic direct red dye from aqueous solutions. Experimental data were consistent with Freundlich isotherm and adsorption capacity was reported 70 mg/g for the dye at 60°C (19). Zhu et al. reported that separation efficiency could get close to 90% for carcinogenic dyes from aqueous solutions using chitosan adsorbents modified by magnetic carbon nanotubes. Adsorption capacity was calculated 262 mg/g (20). Finally, Fazelirad et al. studied the removal of amoxicillin using MMWCNTs. The highest uptake occurred at about pH = 6.4 in presence of a high adsorbent dosage. The bonding between amoxicillin and adsorbent was due to the van der Waals force and adsorption conformed to Langmuir isotherm (21).

Herein, multi-walled carbon nanotubes were first magnetized. Afterward, the modified adsorbent was characterized by means of XRD analysis and FTIR. In the next step, SDS removal was investigated using MMWCNTs. The effects of SDS concentration, pH values, and adsorbent dosage were investigated on SDS removal from aqueous solutions using MMWCNTs. The results indicated that adsorbent used in the present study had remarkable adsorption capability for SDS removal. As a final point, it is worth noting that after adsorption process, adsorbent can be easily separated from the aqueous solution without introducing any secondary pollutant to the solution merely by applying a magnetic field.

2. Methods

2.1. Chemicals

MWCNT ($\geq$ 95%) was purchased from SKC (England) and sodium dodecyl sulfate (SDS) ($\geq$ 99%) was prepared from HACH (Germany) and used as received. Other chemicals such as $FeSO_4.7H_2O$ were provided from Merck (Germany) and all other chemicals were of analytical grade. Typical properties of SDS and MWCNTs are listed in Table 1. Chemical structure of SDS is shown in Figure 1.

2.2. Synthesis of Fe3O4/MWCNTs Nanocomposite

100 mg MWCNTs were added to a flask containing 120 mL mixture of H_2SO_4/HNO_3 (3:1, v/v). The mixture was refluxed at 60°C in an ultrasonic bath (50 kHz and 350 W) for 3 hours. The obtained mixture was filtered and washed with deionized water for several times. Afterwards, the modified MWCNTs were dried at 80°C under vacuum for 8 hours. The as-treated MWCNTs were suspended in 500 mL deionized water. From this step onwards, magnetization procedure has been described.

Table 1. Typical Properties of Sodium Dodecyl Sulfate (SDS) and Magnetic Multi-Walled Carbon Nanotubes (MMWCNTs)

MMWCNTs		SDS	
Outer diameter, nm	20 - 30	Chemical Structure	$NaC_{12}H_{25}SO_4$
Length, μm	30	Molecular weight, g/mol	288.372
Specific surface area, m^2	110	Appearance	White powder
Density, g/cm^3	1.2	Density, g/cm^3	1.01

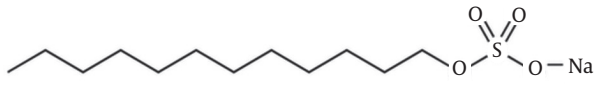

Figure 1. Chemical structure of Sodium Dodecyl Sulfate (SDS)

30 mL MWCNTs were poured dropwise into a 250 mL flask containing 100 mL deionized water. In order to get rid of dissolved oxygen, the solution was bubbled with N_2 flow for 15 minutes. The flask was placed in a 95°C water bath and then 2 g $FeSO_4.7H_2O$ was added to the flask. Ultimately, 40 mL solution of 1.8 g NaOH and 0.9 g $NaNO_3$ was heated up to 95°C and poured dropwise (2 mL/min) into the heating MWCNTs-metal solution. It is worth noting that the solution was stirred vigorously under N_2 flow during reaction period. The final solution was heated up to 95°C for 2 hours and then cooled to the ambient temperature. The precipitates were separated from the flask using a magnetic field. In order to dry the formed Fe_3O_4/MWCNTs nanocomposites, they were placed into a vacuum oven at 100°C for 24 hours (22).

2.3. Characterization Methods

X-ray diffraction (Philips PW1800) was carried out to evaluate the crystalline structure of synthesized products. In addition, Fourier transform infrared spectroscopy (FTIR) (Perkin Elmer Co. USA) analysis was recorded in the range of 400 - 4000 cm^{-1} to assess the functional groups of MWCNTs and MMWCNTs.

2.4. Batch Adsorption Studies

Adsorbent dosage, pH, and SDS concentration were parameters examined in this study. In order to ensure re-

peatability of results, all tests were performed two times and the average values were reported. A stock solution of SDS (500 mg/L) was prepared by dissolving 0.5 g SDS in 1 L deionized water. Solutions containing the desired concentration of SDS were prepared by diluting the stock solution with deionized water. pH of solution was adjusted using 0.1 M sodium hydroxide or sulfuric acid using a digital pH meter (HACH Sension 4).

In order to determine SDS concentration, methylene blue active substance (MBAS) method was followed. In this method, 10 mL of sulfate buffer was added to 300 mL SDS solution. The obtained solution was stirred for 5 minutes. In the next step, the contents of one detergent reagent powder pillow and 30 mL toluene were added to the solution. Contents of flask were shaken gently for 1 minute. Finally, the solution was poured into a decantation funnel and remained immobile for 30 minutes until two different phases appeared separately. Then, the bottom phase was discharged and the upper phase was poured into a 10 mL cell holder. The detergent concentration was read at a wavelength of 652 nm using a DR5000 (HACH) spectrophotometer (23). The following equations were used to determine the adsorbent removal efficiency:

$R = (C_0 - C_e)/C_0$ (1)

C_0 and C_e are the initial and the final concentrations of surfactant (mg/L) (SDS concentration before and after adsorption), respectively. Surfactant adsorption capacity was calculated using the following equation:

$q_e = (C_0 - C_e)V/W$ (2)

qe is the adsorbate concentration per adsorbent mass (mg/g), V is the volume of reactor (L), and W is mass of adsorbent (g).

3. Results and Discussion

3.1. Characterization

FTIR spectra of MWCNTs and MMWCNTs are shown in Figure 2. In the MWCNTs curve, bands at 2919.57 cm^{-1} and 3434 cm^{-1} stand for stretching vibration of -CH and -OH, respectively (24). In fact, the broad peak at 3434 cm^{-1} can be attributed to the moisture adsorbed on the adsorbent or it may stand for OH bond of carboxylic acid. The reason why S = O and N = O peaks of modified adsorbents at 1131 cm^{-1}, 1448 cm^{-1}, and 1636 cm^{-1} bands are stronger than those of unmodified ones is due to the use of nitrogen and sulfate compounds in the synthesis of MMWCNTs. The band at 579 cm^{-1} confirms the presence of stretching vibration of Fe-O in crystal lattice of Fe_3O_4 in MMWCNTs (25).

FTIR spectrum of the MMWCNTs after SDS adsorption is exhibited in Figure 3. As can be observed, there are some prominent peaks described as follows:

Hydrocarbon chains of SDS (C-H) are capable of producing peaks in the range from 1300 cm^{-1} to 1400 cm^{-1}, so the peak at 1383.85 cm^{-1} can be attributed to C-H bonds (26, 27). The band at 1457.3 cm^{-1} indicates C-H2 bonds of SDS. The bands at 976.9 cm^{-1} and 1250 cm^{-1} represent symmetric and asymmetric stretching of S = O bonds, respectively. It is evident that, SDS was adsorbed successfully by MMWCNTs due to the presence of S = O bands in FTIR curve (28). As mentioned earlier, bands at 3434 cm^{-1} and 2919 cm^{-1} can be attributed to the moisture adsorbed on the adsorbent.

Figure 4 shows the XRD patterns of MWCNTs and MMWCNTs in the range of 2θ = 15 - 65°. According to the modified modified nanocomposite has high magnetic properties in comparison with unmodified one, may be due to the periodic arrangement of the crystalline phase and the high percentage of iron (Fe_3O_4) within MMWCNTs. As can be observed in Figure 4 (MWCNTs XRD pattern), the peak at 44° stands for crystalline diffraction and regular arrangement of concentric cylinders of carbon atoms (29). Regarding the XRD pattern of MMWCNTs, the maximum peak appeared at 27° with intensity of 203.0965. The mentioned peak symbolizes cubic crystals of FeSO4.7H2O. Consequently, the XRD analysis confirmed the presence of iron in the magnetic nanocomposite structure (30).

Figure 5 shows the XRD pattern of MMWCNTs after SDS adsorption in the range of 2θ = 15 - 65°. In addition to the peaks observed in the crystal structure of carbon nanotubes and cubic crystals of iron sulfate, a peak appearing at 36° represents reflections of the lamellar phase constructed by mixture of SDS (27).

3.2. Adsorption Studies

3.2.1. Adsorption Isotherm

The adsorption isotherm is an equation relating to the amount of solute adsorbed onto the solid and the equilibrium concentration of the solute in solution at a given temperature (31). Equilibrium data can be analyzed using several well-known adsorption isotherms. There are several models for predicting the equilibrium distribution. However, the following models are most commonly used. The Freundlich, Langmuir, and Sips models were employed to analyze the adsorption process. The Langmuir model describes quantitatively the formation of a monolayer adsorbate on the outer surface of the adsorbent and after that, no further adsorption takes place. The linear equation is as follows:

$1/q_e = 1/(q_{max}) + 1/(bq_{max}C_e)$ (3)

Where q_e is the amount of adsorbed mass per unit weight of adsorbent (mg/g), Ce the equilibrium concentration (mg/L), qmax the maximum adsorption capacity (mg/g), and b is the equilibrium constant related to the free

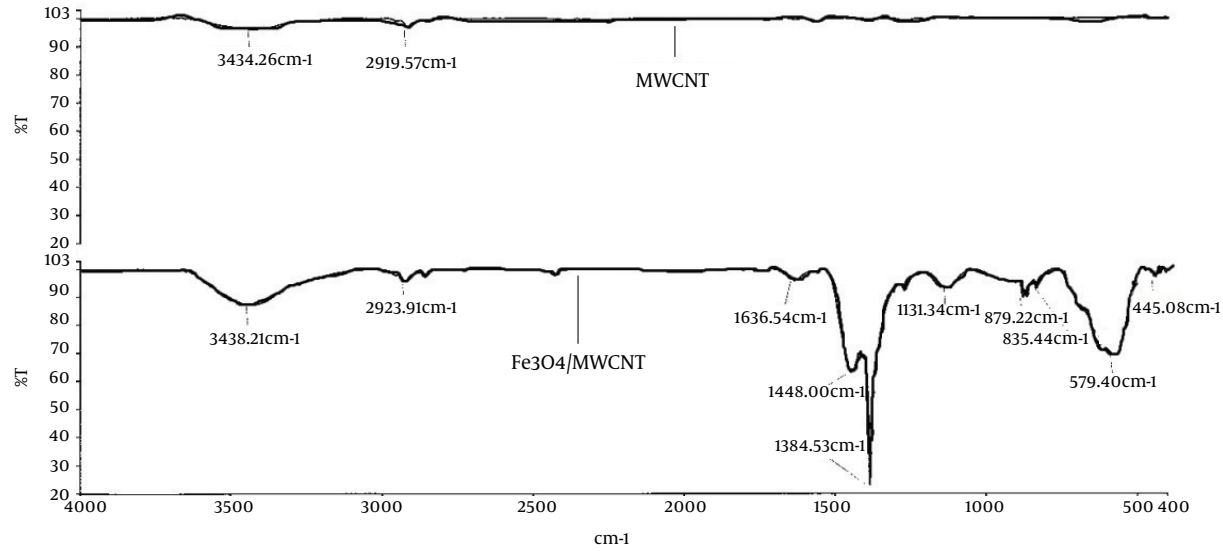

Figure 2. FTIR Spectra of MWCNTs and MMWCNTs

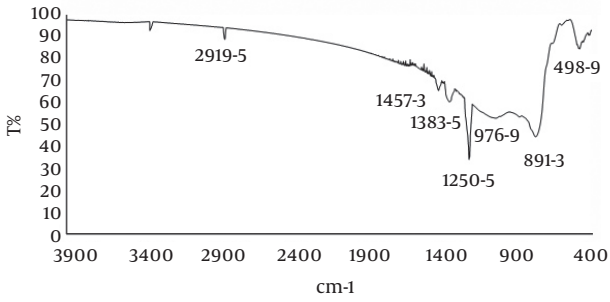

Figure 3. FTIR Spectra of MMWCNTs after SDS Adsorption

energy of adsorption. Freundlich adsorption isotherm is commonly used to describe the adsorption characteristics for heterogeneous surfaces. These data often are fitted to the empirical equation proposed by Freundlich:

$$\text{Log } q_e = \text{Log } K_f + (1/n)\text{Log } C_e \quad (4)$$

Where q_e is the amount of adsorbed mass per unit weight of adsorbent (mg/g), C_e is the equilibrium concentration (mol/L), k_f is the constant expressing the relative adsorption capacity of the adsorbent (mg/g (mg/L) n), and 1/n is the constant expressing the intensity of the adsorption.

The Sips model is an experimental model obtained from combination of the Langmuir and Freundlich adsorption models. The Sips model contains three parameters, q_{max}, KS, and 1/n, which can be assessed by fitting the experimental data. The Sips adsorption isotherm is written as follows:

$$Q_e = (q_{max}\ KS/(1 + KS)\ (5)$$

Where the symbols have the same meanings as previously described. For SDS adsorption studies, 0.5 g adsorbent was added to 300 mL solutions containing various SDS concentrations. The experiments revealed that the equilibrium time was about 120 minutes. Figure 6 provides a comparison between the experimental and isotherms data (32). Parameters of the three isotherms for SDS adsorption using MMWCNTs are shown in Table 2. As can be seen, the highest regression (R^2) values are 0.99 and 0.993 for the Sips and Langmuir models, respectively. Therefore, the experimental data were better described by the Langmuir model (32).

Table 2. Parameters of Different Isotherm Models for SDS Adsorption Using MMWCNTs

Sips Model	Freundlich Model	Langmuir Model
q_{max} (mg g^{-1})= 51	KF (mg g^{-1}(mg L^{-1})$^{-1/n}$)= 6.23	q_{max} (mg g^{-1}) = 61
K_s = 0.1	N = 1.9	KL (L mg^{-1})= 0.07
R^2 = 0.99	R^2 = 0.98	R^2 = 0.993

Table 3 makes a comparison between adsorption capacities of various adsorbents applied to remove SDS. Apart from Chitosan hydrogel beads, MMMCNTs have by far the highest capacity compared to other adsorbents. Hence, this adsorbent, owing to the lower amount of adsorbent needed to remove contaminants, has high efficiency for SDS removal.

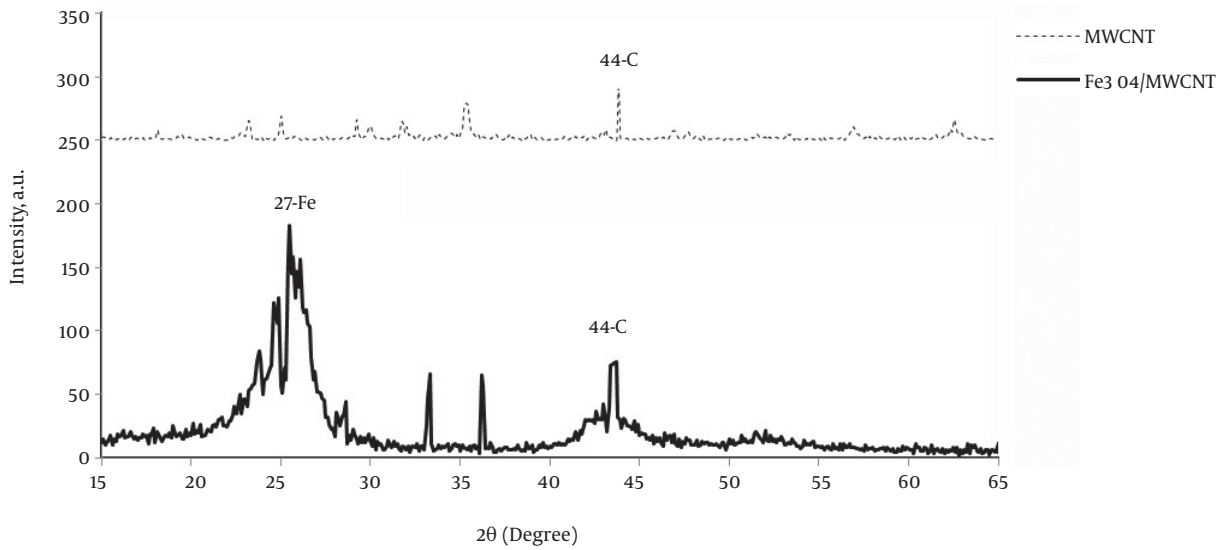

Figure 4. XRD Patterns of MWCNTs and MMWCNTs

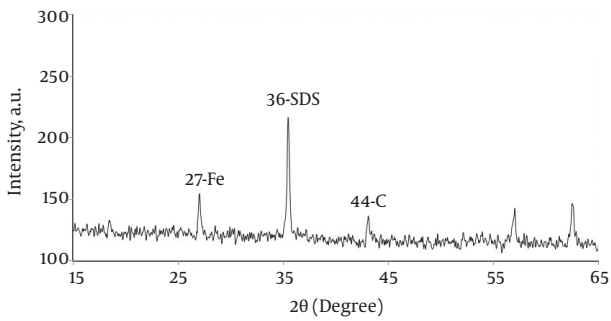

Figure 5. XRD Patterns of MMWCNTs After SDS Adsorption

Table 3. Comparative Analysis for the Removal of Surfactants Using Various Adsorbents

Adsorbent	Surfactant Adsorption Capacity, mg/g	References
Partial template-containing MCM-41	39.9	(32)
Chitosan hydrogel beads	76	(33)
Alumina	39.6	(34)
Wood charcoal	3.75	(35)
Rubber granules	4.1	(35)
Silica gel	5.2	(35)
MMWCNTs	61	This work

3.2.2. Adsorption Kinetics

In order to investigate the rate of SDS adsorption, the Lagergren equation as one of the renowned equations was applied. The pseudo first order kinetic model of Lagergren can be symbolized as follows:

$dq_t/q_t = k_1(q_e\text{-}q_t)$ (6)

Where q_e and q_t are the amounts of adsorbate (mg/g) at equilibrium time and specific time t (min), respectively. Besides, k1 is the rate constant of pseudo-first-order adsorption (min^{-1}). The pseudo second order equation dependent upon adsorption equilibrium capacity can be represented as follows:

$dq_t/q_t = k_2(q_e\text{-}q_t)^2$ (7)

Where q_e and q_t have the same meanings as mentioned earlier and K^2 is the pseudo second order rate constant ($g/mg\ min^{-1}$).

Figure 7 depicts the effect of time on the adsorption capacity of SDS from aqueous solutions at room temperature. An increase in contact time (from 10 to 180 minutes) led to the gradual improvement in adsorption capacity of adsorbent that may be due to the use of all adsorbent sites over a long period. After reaching the equilibrium time (120 minutes), the equilibrium state was established between adsorbent (MMWCNTs) and adsorbate (SDS) (18, 19). No significant changes in SDS adsorption were observed after the equilibrium time. In order to investigate SDS adsorption at different times and determine adsorption rates, the pseudo second order model that was consistent with experimental data was used. Results of the

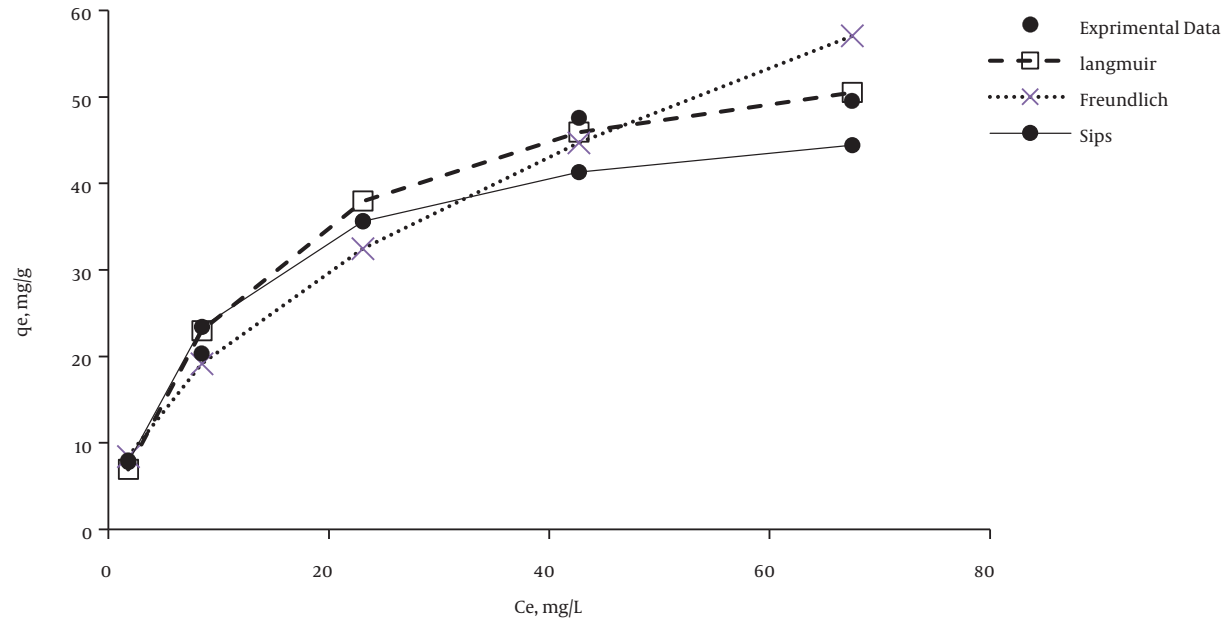

Figure 6. The Comparison of Experimental Adsorption Data with Langmuir, Freundlich, and Sips Models for SDS Adsorption Using MMWCNTs

adsorption kinetics are shown in Table 4.

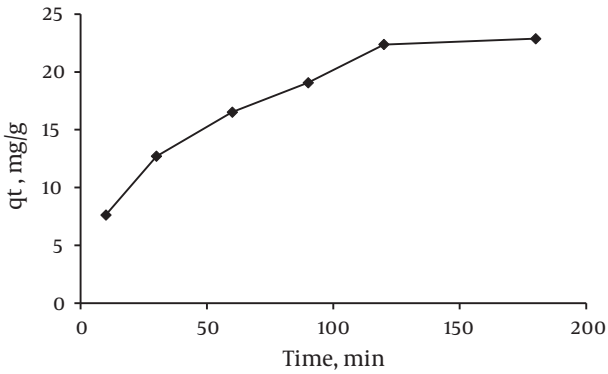

Figure 7. SDS Uptake Kinetics Using MMWCNTs

Table 4. Adsorption Parameters Related to the Pseudo First- and Second-Order Equations

Pseudo First-Order Equation	Pseudo Second-Order Equation
q_e (mg g^{-1}) = 19	q_e (mg g^{-1}) = 27
K (mg g^{-1} h^{-1}) = 0.0167	K (mg g^{-1} h^{-1}) = 0.0016
R^2 = 0.96	R^2 = 0.992

3.3. Optimization of Operating Parameters

The impacts of independent variables such as pH, SDS concentration, and adsorbent dosage on SDS removal were studied. Adsorption capacity of MMWCNTs for SDS adsorption was also evaluated and the response was reported as the percentage of SDS removal. In order to achieve the optimal SDS adsorption capacity, the time of adsorption process was considered 120 minutes. The results showed that the maximum SDS adsorption occurred at pH < 4.56, low SDS concentration, and high dosage of adsorbent.

3.3.1. Effect of pH

pH has a significant impact on SDS adsorption that can be interpreted based on the characteristics of surfactant ionization. In addition, one of the most important features of adsorbent is pHzpc that represents the distribution of electric charge on the adsorbent surface. When pH value is higher than pHzpc, dominant electronic charge on the adsorbent surface is negative and vice versa. The pHzpc values of MWCNTs and MMWCNTs are 5.9 and 4.7, respectively (33). Therefore, in acidic values, dominant electronic charge on the adsorbent surface is positive. In acidic pH, SDS adsorption efficiency was higher than in alkaline values (Figure 8). The highest adsorption rate was reported at pH = 4, and an increment in pH led to a decrement in adsorption rate. Presence of electrostatic force between the positive charge on the surface of adsorbent and negative charge on the anionic surfactant (SDS) may be a rea-

son for the rise in SDS adsorption. Moreover, in acidic pH, the connection between hydrophobic chains of the surfactant and adsorbent will improve, while in alkaline pH due to the presence of OH- groups, a competition will arise between these groups and the anionic surfactant for adsorbing on the surface of positively charged adsorbent and thus, a remarkable reduction in adsorption efficiency will be observed (3, 36).

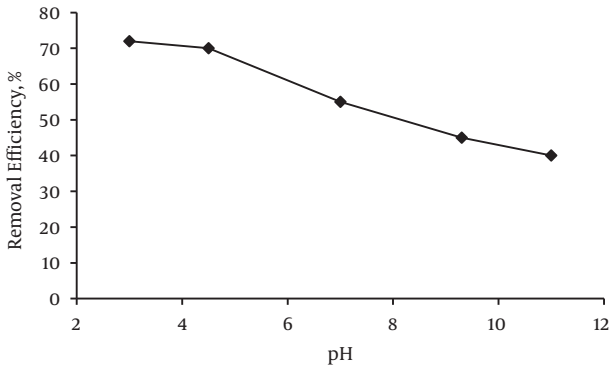

Figure 8. Effect of pH on SDS Adsorption Onto MMWCNTs

3.3.2. Effect of Adsorbent Dosage

In order to evaluate the effect of adsorbent concentration, a wide range of concentrations (from 0.05 to 0.5 g/L) was selected. The effects of adsorbent concentration on SDS adsorption efficiency are exhibited in Figure 9. A rise in adsorbent concentration and thereby an increase in the available adsorption sites of adsorbents led to the enhancement of adsorption efficiency (37). Given that MWCNTs is a hydrophobic adsorbent, the hydrophobic sections of SDS can easily adsorb to the adsorbent sites (36). It should be noted that the influence of independent variables on MWCNTs were studied, as well. The results of SDS removal using MWCNTs are similar to outcomes reported using MMWCNTs for SDS adsorption. The difference between MWCNTs and MMWCNTs is that the specific surface of magnetized adsorbent, due to the presence of iron on the surface of modified adsorbent, is slightly less that pristine adsorbent. Therefore, the reduction in specific surface of MMWNCTs could contribute to the slight decline in MMWCNTs adsorption efficiency. It is worth noting that in acidic conditions, there is a possibility of iron oxides separation from adsorbent surface that is normally negligible and cannot affect adsorption efficiency. With regard to the easy separation of the magnetic adsorbents from aqueous solutions, using a magnetic field is strongly recommended (17, 18). In short, in Figure 9, data regarding the use of MMWCNTs are just reported.

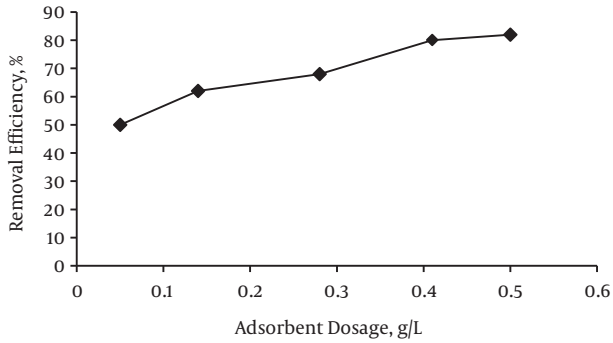

Figure 9. Effect of Adsorbent Dosage on SDS Adsorption on MMWCNTs

3.3.3. Effect of SDS Concentration

In order to evaluate the effect of SDS concentration on adsorption efficiency, a wide range of concentrations (from 15 to 150 mg/L) was considered. The effects of SDS concentration on adsorption efficiency are shown in Figure 10. As can be observed, an increase in SDS concentration led to a decline in adsorption efficiency that may be due to the saturation of adsorption sites. Moreover, when SDS concentration is high, repulsive forces between SDS molecules will rise and this problem prevents SDS from adsorption on the adsorbent (38). Therefore, by increasing SDS concentration (from 15 to 150 mg/L) adsorption efficiency gradually decreased. On the other hand, the amount of adsorbed SDS on adsorbent increased. Indeed, this is due to the intensification of driving forces. As a result, by increasing SDS concentration gradient, SDS adsorption on adsorbent will improve. Finally, when SDS concentration is low, the ratio of SDS molecules to the available adsorption sites is low, too. However, in high SDS concentrations, available adsorption sites are not sufficient to adsorb SDS molecules and thus, SDS removal depends on the initial concentration of the solution (33).

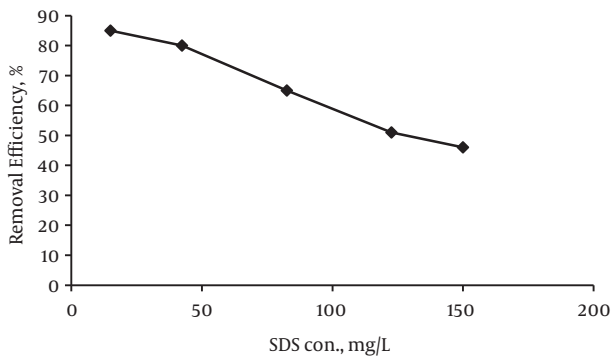

Figure 10. Effect of SDS Concentration on SDS Adsorption Onto MMWCNTs

3.4. Desorption Study

After adsorption of pollutant (SDS), the regeneration of adsorbent was carried out. For this purpose, the adsorbents (MMWCNTs after SDS adsorption) were placed into alkaline aqueous solutions (pH 10.0 - 14.0) for 24 hours. During this process, just about 15% of adsorbed SDS was released into the alkaline solution. Indeed, desorption of anionic SDS molecules into the solution took place gradually. This confirms the earlier conclusion explaining that SDS adsorption on MMWCNTs is due to both ionic and hydrophobic interactions between MMWCNTs and SDS molecules (33, 36).

4. Conclusions

MMWCNTs were synthesized to combine distinguishing characteristics of MWCNTs and magnetic properties. FTIR and XRD analysis demonstrated that SDS was adsorbed on MMWCNTs. After 120 min, the equilibrium occurred and kinetics of pseudo second order model was consistent with the experimental results. Langmuir and Sips isotherms showed the highest correlation coefficient with SDS removal. The maximum SDS adsorption capacity was calculated about 61 mg/g. Based on the results achieved in this study, MMWCNTs showed an acceptable behavior towards SDS removal. Generally, MMWCNTs are an appropriate adsorbent for SDS removal, and due to their relatively high adsorption capacity, they are capable of removing environmental pollutions. More importantly, magnetized adsorbents can easily separate from aqueous solutions using a magnetic field.

Acknowledgments

The authors gratefully acknowledge Hamadan University of Medical Sciences for financial support (grant No. 9212134272). We would like to pay homage to those who have contributed to the present study.

References

1. Mendez-Paz D, Omil F, Lema JM. Anaerobic treatment of azo dye Acid Orange 7 under fed-batch and continuous conditions. *Water Res.* 2005;**39**(5):771–8. doi: 10.1016/j.watres.2004.11.022. [PubMed: 15743621].
2. Rahimi K, Adibifard M. Experimental Study of the Nanoparticles Effect on Surfactant Absorption and Oil Recovery in One of the Iranian Oil Reservoirs. *Petroleum Sci Technol.* 2014;**33**(1):79–85. doi: 10.1080/10916466.2014.950382.
3. Beltran-Heredia J, Sánchez-Martín J, Barrado-Moreno M. Long-chain anionic surfactants in aqueous solution. Removal by Moringa oleifera coagulant. *Chem Engin J.* 2012;**180**:128–36. doi: 10.1016/j.cej.2011.11.024.
4. Zhong X, Duan F. Surfactant-Adsorption-Induced Initial Depinning Behavior in Evaporating Water and Nanofluid Sessile Droplets. *Langmuir.* 2015;**31**(19):5291–8. doi: 10.1021/acs.langmuir.5b00288.
5. Yavuz R, Küçükbayrak S. Adsorption of an anionic dispersant on lignite. *Energy Conversion Manag.* 2001;**42**(18):2129–37. doi: 10.1016/s0196-8904(00)00169-2.
6. Paria S, Khilar KC. A review on experimental studies of surfactant adsorption at the hydrophilic solid-water interface. *Adv Colloid Interface Sci.* 2004;**110**(3):75–95. doi: 10.1016/j.cis.2004.03.001. [PubMed: 15328059].
7. Pham TD, Kobayashi M, Adachi Y. Adsorption of anionic surfactant sodium dodecyl sulfate onto alpha alumina with small surface area. *Colloid Polymer Sci.* 2014;**293**(1):217–27. doi: 10.1007/s00396-014-3409-3.
8. Li Z, Yuansheng D, Hanlie H. Transport of micelles of cationic surfactants through clinoptilolite zeolite. *Microporous Mesoporous Materials.* 2008;**116**(1-3):473–7. doi: 10.1016/j.micromeso.2008.05.006.
9. Trojanowicz M. Analytical applications of carbon nanotubes: a review. *TrAC Trends Analyt Chem.* 2006;**25**(5):480–9. doi: 10.1016/j.trac.2005.11.008.
10. Upadhyayula VK, Deng S, Mitchell MC, Smith GB. Application of carbon nanotube technology for removal of contaminants in drinking water: a review. *Sci Total Environ.* 2009;**408**(1):1–13. doi: 10.1016/j.scitotenv.2009.09.027. [PubMed: 19819525].
11. Thavorn J, Hamon JJ, Kitiyanan B, Striolo A, Grady BP. Competitive surfactant adsorption of AOT and Tween 20 on gold measured using a quartz crystal microbalance with dissipation. *Langmuir.* 2014;**30**(37):11031–9. doi: 10.1021/la502513p. [PubMed: 25158240].
12. Perez-Aguilar NV, Diaz-Flores PE, Rangel-Mendez JR. The adsorption kinetics of cadmium by three different types of carbon nanotubes. *J Colloid Interface Sci.* 2011;**364**(2):279–87. doi: 10.1016/j.jcis.2011.08.024. [PubMed: 21924733].
13. Lu C, Chiu H. Adsorption of zinc(II) from water with purified carbon nanotubes. *Chem Engin Sci.* 2006;**61**(4):1138–45. doi: 10.1016/j.ces.2005.08.007.
14. Gupta VK, Agarwal S, Saleh TA. Chromium removal by combining the magnetic properties of iron oxide with adsorption properties of carbon nanotubes. *Water Res.* 2011;**45**(6):2207–12. doi: 10.1016/j.watres.2011.01.012. [PubMed: 21303713].
15. Iijima S. Helical microtubules of graphitic carbon. *Nature.* 1991;**354**(6348):56.
16. Yu F, Chen J, Chen L, Huai J, Gong W, Yuan Z, et al. Magnetic carbon nanotubes synthesis by Fenton's reagent method and their potential application for removal of azo dye from aqueous solution. *J Colloid Interface Sci.* 2012;**378**(1):175–83. doi: 10.1016/j.jcis.2012.04.024. [PubMed: 22564767].
17. Gao H, Zhao S, Cheng X, Wang X, Zheng L. Removal of anionic azo dyes from aqueous solution using magnetic polymer multi-wall carbon nanotube nanocomposite as adsorbent. *Chem Engin J.* 2013;**223**:84–90. doi: 10.1016/j.cej.2013.03.004.
18. Tang WW, Zeng GM, Gong JL, Liu Y, Wang XY, Liu YY, et al. Simultaneous adsorption of atrazine and Cu (II) from wastewater by magnetic multi-walled carbon nanotube. *Chem Engin J.* 2012;**211-212**:470–8. doi: 10.1016/j.cej.2012.09.102.
19. Konicki W, Pełech I, Mijowska E, Jasińska I. Adsorption of anionic dye Direct Red 23 onto magnetic multi-walled carbon nanotubes-Fe3C nanocomposite: Kinetics, equilibrium and thermodynamics. *Chem Engin J.* 2012;**210**:87–95. doi: 10.1016/j.cej.2012.08.025.
20. Zhu HY, Fu YQ, Jiang R, Yao J, Liu L, Chen YW, et al. Preparation, characterization and adsorption properties of chitosan modified magnetic graphitized multi-walled carbon nanotubes for highly effective removal of a carcinogenic dye from aqueous solution. *Appl Surface Sci.* 2013;**285**:865–73. doi: 10.1016/j.apsusc.2013.09.003.
21. Fazelirad H, Ranjbar M, Taher MA, Sargazi G. Preparation of magnetic multi-walled carbon nanotubes for an efficient adsorption and spectrophotometric determination of amoxicillin. *J Indust Engin Chem.* 2015;**21**:889–92. doi: 10.1016/j.jiec.2014.04.028.

22. Hu X, Liu B, Deng Y, Chen H, Luo S, Sun C, et al. Adsorption and heterogeneous Fenton degradation of 17α-methyltestosterone on nano Fe3O4/MWCNTs in aqueous solution. *Appl Catalysis B Environ.* 2011;**107**(3-4):274–83. doi: 10.1016/j.apcatb.2011.07.025.
23. Llenado RA, Neubecker TA. Surfactants. *Analyt Chem.* 2002;**55**(5):93–102. doi: 10.1021/ac00256a008.
24. Misra A, Tyagi PK, Rai P, Misra DS. FTIR Spectroscopy of Multiwalled Carbon Nanotubes: A Simple Approachto Study the Nitrogen Doping. *J Nanosci Nanotechnol.* 2007;**7**(6):1820–3. doi: 10.1166/jnn.2007.723.
25. Li H, Wan J, Ma Y, Wang Y, Huang M. Influence of particle size of zero-valent iron and dissolved silica on the reactivity of activated persulfate for degradation of acid orange 7. *Chem Engin J.* 2014;**237**:487–96. doi: 10.1016/j.cej.2013.10.035.
26. Viana RB, da Silva ABF, Pimentel AS. Adsorption of Sodium Dodecyl Sulfate on Ge Substrate: The Effect of a Low-Polarity Solvent. *Int J Mol Sci.* 2012;**13**(12):7980–93. doi: 10.3390/ijms13077980.
27. Ramimoghadam D, Hussein M, Taufiq-Yap Y. The Effect of Sodium Dodecyl Sulfate (SDS) and Cetyltrimethylammonium Bromide (CTAB) on the Properties of ZnO Synthesized by Hydrothermal Method. *Int J Mol Sci.* 2012;**13**(12):13275–93. doi: 10.3390/ijms131013275.
28. Viana RB, da Silva ABF, Pimentel AS. Infrared spectroscopy of anionic, cationic, and zwitterionic surfactants. *Adv Phys Chem.* 2012;**2012**.
29. Zhang Y, Xiao S, Wang Q, Liu S, Qiao Z, Chi Z, et al. Thermally conductive, insulated polyimide nanocomposites by AlO(OH)-coated MWCNTs. *J Materials Chem.* 2011;**21**(38):14563. doi: 10.1039/c1jm12450a.
30. Sui M, Xing S, Sheng L, Huang S, Guo H. Heterogeneous catalytic ozonation of ciprofloxacin in water with carbon nanotube supported manganese oxides as catalyst. *J Hazard Materials.* 2012;**227-228**:227–36. doi: 10.1016/j.jhazmat.2012.05.039.
31. Arasteh R, Masoumi M, Rashidi AM, Moradi L, Samimi V, Mostafavi ST. Adsorption of 2-nitrophenol by multi-wall carbon nanotubes from aqueous solutions. *Appl Surface Sci.* 2010;**256**(14):4447–55. doi: 10.1016/j.apsusc.2010.01.057.
32. Ariapad A, Zanjanchi MA, Arvand M. Efficient removal of anionic surfactant using partial template-containing MCM-41. *Desalination.* 2012;**284**:142–9. doi: 10.1016/j.desal.2011.08.048.
33. Pal A, Pan S, Saha S. Synergistically improved adsorption of anionic surfactant and crystal violet on chitosan hydrogel beads. *Chem Engin J.* 2013;**217**:426–34. doi: 10.1016/j.cej.2012.11.120.
34. Raval Priti V, Desai Hemangi H. Removal of anionic surfactant sodium dodecyl sulphate (SDS) from aqueous solution by using alumina. *J Environ Res Dev Vol.* 2012;**7**(2A).
35. Purakayastha PD, Pal A, Bandyopadhyay M. Adsorbent selection for anionic surfactant removal from water. *Indian J Chem Technol.* 2005;**12**(3):281–4.
36. Ncibi MC, Gaspard S, Sillanpaa M. As-synthesized multi-walled carbon nanotubes for the removal of ionic and non-ionic surfactants. *J Hazard Materials.* 2015;**286**:195–203. doi: 10.1016/j.jhazmat.2014.12.039.
37. Islam MF, Rojas E, Bergey DM, Johnson AT, Yodh AG. High Weight Fraction Surfactant Solubilization of Single-Wall Carbon Nanotubes in Water. *Nano Lett.* 2003;**3**(2):269–73. doi: 10.1021/nl025924u.
38. Kaya Y, Gönder ZB, Vergili I, Barlas H. Removal of cetyltrimethylammonium bromide and sodium dodecylether sulfate by granular activated carbon. *J Sci Indust Res.* 2008;**67**(3):249.